Estimation of Surface Roughness in Selective Laser Sintering Using Computational Models

Ebubekir Koç (ekoc@fsm.edu.tr)
Fatih Sultan Mehmet Vakıf Üniversitesi https://orcid.org/0000-0002-9069-715X
Sultan Zeybek
Burçin Özbay Kısasöz
Cemal İrfan Çalışkan
M. Enes Bulduk

Research Article

Keywords: Advanced Manufacturing, Additive Manufacturing, Selective Laser Sintering, Surface Roughness, Artificial Intelligence, Deep Neural Networks

Posted Date: June 9th, 2022

DOI: https://doi.org/10.21203/rs.3.rs-1638732/v1

Abstract

In this study, a novel classification model is proposed to estimate surface roughness for the parts produced in an industrial additive manufacturing technology. The proposed model focused on selective laser sintering (SLS) technology based on polyamide 12 powder applications. A comprehensive dataset is designed to simulate the production parts and manufactured at an industrial SLS machine based on a proposed positioning strategy and random positions to test the robustness of the dataset and the model. The proposed classification model is based on Deep Neural Networks (DNN) with hyperparameters designed for the problem. Benchmark results show that the model outperforms other machine learning methods on classifying the surface roughness successfully on the test dataset. The dataset and the model provide a new user interface to estimate the surface roughness depending on the coordinates of a given product surface in a SLS production chamber and the production parameters employed in the production planning phase.

1. Introduction

In recent years, advanced manufacturing technologies have increasingly adopted artificial intelligence for more efficient and robust manufacturing. Ensuring the high-quality output in the production planning phase in additive manufacturing is a labour-intensive task. Especially in selective laser sintering (SLS) and direct metal laser sintering (DMLS) technologies, the position of the part has a significant effect on surface roughness, and it needs a high level of human expertise to estimate the surface roughness, which directly affects the quality of the final product.

Additive Manufacturing (AM) technologies are methods that enable the rapid production of three-dimensional complex-shaped parts. They can be worked with wax, ceramics, polymers, metals, and biomaterials. Different types of raw materials in powder, sheet, filament and liquid are available. In all AM methods, parts using computer-aided design (CAD) are produced by depositing the material layer by layer through selective fusion, sintering, or polymerisation [1, 2].

SLS technologies are generally used for rapid prototyping in their early stages. However, in recent years, the technology is also implemented for mass production when materials are available and cost-effective for the given application. The SLS deploys a powder bed technology approach as part of additive manufacturing. Since the manufacturing is focused on layer-based laser sintering, the technology may employ several different layer thicknesses (60µm, 100µm, 120µm) depending on applications, surface quality and material properties [3, 4, 5].

Production procedures can be explained as follows: First, the powder is spread to the production area by the recoater or blade as much higher as the production layer thickness. The design section of the first layer is scanned and melted by an optical laser. In the second stage, the production platform lowered to a pre-planned layer thickness, opening the powder feeder required for the next layer. This powder laying and laser sintering continue in loops until the end of the process [6, 7, 8].

The polyamide powder materials cover more than 90% of the thermoplastics at the AM market due to the increasing volumes of PBF machines that use these powders. The polyamide family (Polyamide 12 (PA 12), Polyamide 11 (PA 11, followed by Polyamide 6) is the most widely used thermoplastic polymeric material family. Also, Polypropylene (PP), Polyethylene (PE), Thermoplastic Polyurethane (TPU), Polyetheretherketone (PEEK), Polystyrene (PS) are non-polyamide laser sintering marketing materials [9, 10, 11].

The surface quality of end products can be improved by optimising the process parameters. Bodaghia *et al*. [12] compared the surface quality of printed porous materials produced by SLA, MJF, and FDM 3DP. The benchmark results show that SLA obtained the better surface finish with the lowest standard deviations of roughness. The average roughness (S_a) and root mean square (RSM) roughness (S_q) values of better surface finish of MJF samples are lower than those of FDM. Taufik et al. [13] presented a laser-assisted finishing process to improve FDM parts' surface quality further. The benchmark results showed that when the laser-based finishing process was performed, low arithmetic surface roughness (R_a), negative skewness (R_{sk}) and kurtosis (R_{ku}) > 3 were found as the most appropriate conditions for surface finishing.

In recent years, data-driven solution methods have played a critical role in many engineering problems. They provide better and time-efficient solutions that can extract information from data that might handle the complex nature of the problem, which cannot be solved within a polynomially defined time. Machine learning algorithms and especially deep learning algorithms have been used for many industrial applications, including intelligent damage identification [14], remaining useful life prediction [15], and prediction of energy consumption and surface roughness of the natural materials [16].

Although there are several studies available for enhancing the surface quality in the pre-production (production planning) and post-production phases by optimising the process parameters, there is no research carried out on estimation of surface roughness using a machine learning method and a production dataset that contains positioning and angle values have a substantial effect on the finish surface of final products in SLS systems. Yang *et al.* have proposed a customised method of post-production heating by hybridising material preparation combining properties of the powder and parts. Various combination of the vital process parameters has been investigated using a design of experiments (DoE) method [17]. Caliskan *et al.* have investigated the manufacturability, inner surface properties and efficiency of various geometries conformal cooling channel (CCC) geometries by using direct metal laser sintering (DMLS) system [18].

In this paper, an experimental study is carried out to estimate the surface roughness of any given design during the production planning phase by creating a comprehensive dataset that represents a real production environment with coordinates, angles and observed surface roughness. In section 2, a methodology to prepare an experimental setup and data collection is presented. Experimental setup, effects of standard parameters and a new experimental design are also given. A sample design with four different angles is proposed and manufactured to represent the actual production environment. In section

3, a classification and estimation model is proposed based on deep learning algorithms. In section 4, results of the trained system are presented along with additional benchmarks with other available classification techniques to show the system's robustness.

2. Experimental Setup And Data Collection

2.1. Test Specimen Design

A test specimen is designed in octagonal form with the dimensions of 16mm x 16mm x 18mm (XYZ, respectively), as shown in Fig. 1. The specimen is specially designed to represent actual product conditions with the part design module of Catia V5©. The arrow form in the middle of the test specimen is added to ensure that all samples are produced in the same Z direction relative to X and Y. The size determination of the specimen is limited to the technical specifications of the surface roughness measurement device.

In the SLS production process, certain constraints are considered in the placement of parts throughout the volume of the production chamber. The parts must be separated apart 1mm minimum in the production chamber to achieve standard surface quality, as indicated in the manufacturer's guide. Any contact should result in surface deformation and failure. A minimum of 3mm must be left before the first layer of any product.

The positioning and relative angles of the parts have a substantial effect on the surface quality in the process. In this research, the effects of various parameters on the surface quality are investigated with production samples developed in an octagonal form. It is proposed to create several different angles at the same spot of the production chamber and simulate an actual product with several surfaces simultaneously (see Fig. 1).

A multi-surface octagonal form with various angles on the same sample represents the actual manufacturing conditions. The angles 0^0, 45^0, 90^0 and 135^0 were set relative to *the Z* dimension, as shown in Figs. 2a, 2b, 2c and 2d. The surface roughness measurements to create a dataset are made on these surfaces, as discussed in the following sections. The test samples are positioned in a production volume to gather surface roughness data, as shown in Fig. 3a. A three-dimensional positions data for each sample is recorded, as shown in Fig. 3b.

2.2. Experimental Setup and Process Parameters

Experimental studies are carried out using EOS Formiga P100 machine setup under standard production conditions of temperature, humidity and powder management procedures. The production system is kept in a special environment where EASA Part21 Subpart G civil aviation production organisation approval standards and TS EN ISO 9001:2015 quality management standards are applied. The productions volume of the machine is 192mm, 242mm, 320mm X, Y, Z, respectively, as can be seen in Fig. 3. Surface roughness is measured using the Mitutoyo SJ-500 device.

2.2.1. Preliminary Parameter Determination

In this study, the process parameters that significantly affect surface roughness are studied as preliminary work. It was determined that the standard contour parameters had a more significant effect than on-part and downskin parameters. Standard process chamber temperatures of 168°C and 150°C for the SLS production process was deployed as the building chamber and removal chamber temperatures, respectively. Table 1 presents the constant core parameters of the SLS process and their respected values used throughout the experimental studies.

Table 1
Constant core parameters for EOS P110 Formiga SLS system.

Hatching (Core Parameters)			
Laser Power (W)	**Scan Speed (mm/s)**	**Hatch (mm)**	**Beam Offset**
21	2500	0.25	0.15
Upskin (Core Parameters)			
Laser Power (W)	**Scan Speed (mm/s)**	**Hatch (mm)**	**Thickness (mm)**
21	2500	0.25	0.30
Downskin (Core Parameters)			
Laser Power (W)	**Scan Speed (mm/s)**	**Hatch (mm)**	**Thickness (mm)**
21	2800	0.25	0.30

The preliminary experiments were carried out for only 0^0 and 180^0 surfaces of specimens (see Fig. 1) in the first phase to identify the best set of parameters for dataset creation. Figure 4 presents the mean values of both experimental setups to identify the best possible set compared to the original EOS contour parameters. Table 2 presents the details of the scan and power parameters and their corresponding surface roughness values.

The methodology of the parameter setup is presented in Table 2. In the first stage of parameter trials, the contour parameters given by EOS have been changed. The first stage was completed by increasing and decreasing the scan and power values of the Standard (S_i) parameters in contour. In the first study, six (from S_1 to S_6) contour parameters were determined. The power parameters are adjusted by changing the 2500 mm/s and 800 mm/s max/min scan parameters of the EOS while fixing the 16 W power parameter, and the power parameters are changed from 11 W to 21 W, as max/min values while fixing the 1500 mm/sec scan parameter of the EOS. The min and max values of scan and power parameters used in both cases are also grouped in Table 2 (S_1 to S_6).

Twenty more parameters are created in the second stage of the preliminary study. While the scan value, where the best roughness value is obtained, was kept constant as 800 mm/sec, nine different parameters are tried to observe the effect of the power parameter. Then, while the power value was kept constant as 11 W, the effect of the scan parameter was examined with eleven different parameters. As a result of these experiments, it is determined that the best value is obtained with the S_5 parameter.

As the roughness values of S5, S16 and EOS© parameters are examined in Fig. 5, the best surface roughness values are obtained using the S5 parameter set. Thus, the S5 parameters set are decided as the experimental contour setup and the constant core parameters given in Table 1.

Table 2
Standard contour processing parameters and preliminary experimental mean test results are annotated as S_n containing Scan, Power and corresponding surface roughness values.

	Scan (mm/s)	Power (W)	Surface Roughness (*Ra*)
EOS©	1500	16	11,212
S_1	2500	16	15,657
S_2	800	16	11,106
S_3	1500	11	13,679
S_4	1500	21	12,203
S_5	800	11	10,560
S_6	2500	21	13,967
S_7	1400	11	13,529
S_8	1300	11	13,199
S_9	1200	11	16,004
S_{10}	1100	11	14,633
S_{11}	1000	11	14,449
S_{12}	900	11	15,474
S_{13}	700	11	16,118
S_{14}	600	11	15,886
S_{15}	500	11	14,997
S_{16}	400	11	16,411
S_{17}	300	11	15,820
S_{18}	800	14	15,196
S_{19}	800	13	14,853
S_{20}	800	12	15,240
S_{21}	800	10	13,786

	Scan (mm/s)	Power (W)	Surface Roughness (*Ra*)
S_{22}	800	9	14,449
S_{23}	800	8	13,058
S_{24}	800	7	13,229
S_{25}	800	6	13,718
S_{26}	800	5	12,998

2.3. Experimental Dataset

An experimental dataset is designed to collect data regarding the effect of positioning on surface roughness in the SLS process. Details of the experimental setup and the process parameters used in the experiments are introduced in section 2.2. During dataset creation same setup is used to measure the effect of positioning in a production chamber.

The octagonal test specimen is deployed for the data collection process (see Fig. 1). Three levels of the production chamber (bottom, middle, top) are dedicated to conducting five specimens on each level. In total, fifteen specimens are placed in a production chamber to represent the whole volume (see Fig. 7). The placements are started from 2 mm to 285 mm on the Z coordinates. Table 3 presents the coordinates of each octagonal specimen surface in the process chamber in mm. As shown in Fig. 1, each specimen has four surfaces at 0, 45, 90 and 135 degrees. Table 3 presents the coordinates of central points in each surface of the specimen.

Three more specimens are also designed to test the robustness of the representation of the first set (see Fig. 8). Table 4 presents the coordinates of randomly placed A, B, and C specimens. The test set is also identical to the first batch given in Table 1.

Table 3
XYZ coordinates the octagonal test specimen surfaces in the process chamber (mm).

Sample #1				
	0°	**45°**	**90°**	**135°**
x	8	13.66	16	13.66
y	9	9	9	9
z	2	4.34	10	15.66
Sample #2				
	0°	**45°**	**90°**	**135°**
x	185	190.66	193	190.66
y	9	9	9	9
z	2	4.34	10	15.66
Sample #3				
	0°	**45°**	**90°**	**135°**
x	95,56	101.22	103.56	101.22
y	117,12	117.12	117.12	117.12
z	2	4.34	10	15.66
Sample #4				
	0°	**45°**	**90°**	**135°**
x	8	13.66	16	13.66
y	233	233	233	233
z	2	4.34	10	15.66
Sample #5				
	0°	**45°**	**90°**	**135°**
x	185	190.66	193	190.66
y	233	233	233	233
z	2	4.34	10	15.66
Sample #6				
	0°	**45°**	**90°**	**135°**

Sample #1				
x	8	13.66	16	13.66
y	9	9	9	9
z	142	144.34	150	155.66
Sample #7				
	0°	**45°**	**90°**	**135°**
x	185	190.66	193	190.66
y	9	9	9	9
z	142	144.34	150	155.66
Sample #8				
	0°	**45°**	**90°**	**135°**
x	95.44	101.1	103.44	101.1
y	117.08	117.08	117.08	117.08
z	142	144.34	150	155,66
Sample #9				
	0°	**45°**	**90°**	**135°**
x	8	13.66	16	13.66
y	233	233	233	233
z	142	144.34	150	155.66
Sample #10				
	0°	**45°**	**90°**	**135°**
x	185	190.66	193	190.66
y	232.95	232.95	232.95	232.95
z	142	144.34	150	155.66
Sample #11				
	0°	**45°**	**90°**	**135°**
x	8	13.66	16	13.66
y	9	9	9	9
z	285	287.34	293	298.66

Sample #1				
Sample #12				
	0°	**45°**	**90°**	**135°**
x	185	190.66	193	190.66
y	9	9	9	9
z	285	287.34	293	298.66
Sample #13				
	0°	**45°**	**90°**	**135°**
x	95,37	101.03	103.37	101.03
y	117	117	117	117
z	285	287.34	293	298.66
Sample #14				
	0°	**45°**	**90°**	**135°**
x	8	13.66	16	13.66
y	233	233	233	233
z	285	287.34	293	298.66
Sample #15				
	0°	**45°**	**90°**	**135°**
x	185	190.66	193	190.66
y	233	233	233	233
z	285	287.34	293	298.66

Table 4
Random part positioning in the processing chamber

Sample A				
	0°	**45°**	**90°**	**135°**
x	8	13.66	16	13.66
y	9	9	9	9
z	227	229.34	235	240.66
Sample B				
	0°	**45°**	**90°**	**135°**
x	40.42	46.08	48.42	46.08
y	11.39	11.39	11.39	11.39
z	233.56	235.9	241.56	247.22
Sample C				
	0°	**45°**	**90°**	**135°**
x	86.46	92.12	94.46	92.12
y	81.36	81.36	81.36	81.36
z	233.84	236.18	241.84	247.5

2.4. Characterisation of the Specimens

The surface roughnesses of specimens are measured to complete the dataset. The values were measured using the Mitutoyo SJ-500 surface roughness device. Table 5 presents the surface roughness values of specimens. Table 6 presents the surface roughness values of random positioned samples.

Table 5
Surface roughness values of specimens.

	Surface Roughness (µm)			
Sample Number	**0 °**	**45 °**	**90 °**	**135 °**
1	10.724	13.972	15.867	22.743
2	10.214	11.812	14.842	21.559
3	10.803	12.808	16.229	23.584
4	11.734	12.688	17.029	21.221
5	9.569	12.282	15.668	21.936
6	10.726	13.970	16.178	24.257
7	11.649	13.491	15.882	23.929
8	11.410	14.078	16.114	24.303
9	10.445	13.203	18.677	22.195
10	12.640	15.061	16.999	20.433
11	12.077	13.729	17.623	23.120
12	9.616	13.087	15.941	22.600
13	11.907	13.871	16.160	19.460
14	11.199	13.429	19.386	21.255
15	11.580	13.410	16.096	23.794

Table 6
Surface roughness values of randomly placed specimens.

	Surface Roughness (µm)			
Sample Code	**0 °**	**45 °**	**90 °**	**135 °**
A	11.197	12.785	19.346	21.876
B	11.242	13.686	16.974	23.227
C	13.693	14.856	17.533	23.326

3. Estimation Model

3.1. The Proposed Model

In this study, seven different features, including position x, position y, position z, angle, speed, power, and mixture, have been considered for the classification process of Polyamide 12. The study aims to propose an estimation model to decide whether the surface roughness of the samples is over the threshold in actual production conditions. The average surface roughness, which varies relative to position X, position Y, position Z, and angle value, is used as a decision parameter.

A classification model using a deep neural network (DNN) is proposed in the context of this study. DNN is a well-known artificial neural network model that deploys more than two hidden layers to solve estimation and/or classification problems in many engineering applications that can be solved using a supervised learning algorithm (19). Figure 6 represents an example of a deep learning model with an input layer, three hidden layers, and an output layer. The proposed model has two hidden layers, one drop-out layer and one output layer. The dense layer is modelled with an average value of the surface roughness. The drop-out layer has been used to prevent the overfitting problem.

The transformation between the layers is carried through an activation function. The transformation between layers is defined as follows:

$$z^{(l)} = W^{(l)} . a^{(l-1)}$$

1

Here, $z^{(l)}$ represents the output value for layer l. It is calculated using weight matrix $W^{(l)}$, which is defined by combining an associative weight value $w_{ij}^{(l)}$ from i^{th} neuron of layer $l-1$ to j^{th} neuron of layer l. Learning happens by updating weights using optimisation (training) algorithms. Here $a^{(l)}$ is the activated value of corresponding input value, which is defined using activation function σas follows:

$$a^{(l)} = \sigma\left(z^{(l)}\right)$$

2

Figure 7 presents the proposed pipeline of the estimation/classification model. Details of data cleaning, labelling and pre-processing steps are given in the next section.

3.2. Experimental *Setup*

The dataset is split into training, validation, and test sets (Tables 3, 4, 5 and 6). Ten different deep neural network models have been defined combining different hyper-parameters, given in Table 7. Rectified Linear Unit (ReLU) activation function is used as an activation function combined with Adam optimiser.

Keras Sequential model including dense feature layer is modelled based on the average surface roughness value.

Figure 8 represents the distribution of the roughness measurement of fifteen different samples; each has different positions and angles. In addition to the fifteen different samples, six different samples, which have random positions for each dimension, have also been investigated in terms of surface roughness. Figure 9 represents the distribution of the roughness measurement of the samples, which have random position parameters for each angle, including 0, 45, 90, and 135 degrees.

As it can be seen in Table 7, the reference (threshold) value for the measured surface roughness is defined in two pathways: The first is considering the average value surface roughness measurements of the related angles. The measurement for the EOS sample for each angle, including 0, 45, 90, and 135 degrees, is defined as a reference value to detect the roughness of the related samples. Hence the threshold value of the samples is defined as 10 for angle 0, 12 for angle 45, 15 for angle 90, and 22 for angle 135. The second pathway uses 11 as a standard threshold value for each angle as it is claimed as the threshold value for the default EOS sample with angle 0.

We have proposed two approaches for labelling the data according to these definitions. The first one is labelling the data samples by considering the EOS samples combined with different angles, including 0, 45, 90, and 135 degrees. The dataset samples have been labelled as 'ROUGH' if the surface roughness value is greater than the EOS reference value and as 'SMOOTH' if not. The second approach is labelling the dataset by considering the average threshold value. Since the production temperature of 168°C at 100 µm layer thickness using PA12 powder (PA2200) with EOS P110 Formiga system and standard "Default_EOS" parameter was measured as 11 µm; we claimed the threshold value as 11.

Table 7
Hyper-parameters of the Deep Neural Networks (DNN) model for surface roughness classification using reference value of EOS for different angles.

DNN Model Number	Batch Size	Samples Number of Training /Val. / Test Dataset	Reference Value of EOS for Different Angles (0^o- 45^o- 90^o – 135^o)	Reference Value of EOS	Drop out value	Number of Neurons in Hidden Layers	Number of Epochs
1	2	50 / 6 / 8	10–12 – 15–22	-	0.1	128	100
2	4	40 / 8 / 16	10–12 – 15–22	-	0.1	128	100
3	2	44 / 12 / 8	-	11	0.1	32	100
4	4	40 / 8 / 16	-	11	0.1	64	100
5	2	40 / 8 / 16	-	11	0.1	64	100
6	**-**	**48 / 16**	**-**	**11**	**0.1**	**32**	**100**
7	**-**	**48 / 16**	**10–12 – 15–22**	**-**	**0.1**	**32**	**100**
8	-	48 / 16	-	11	0.1	64	100
9	-	48 / 16	10–12 – 15–22	-	0.1	64	100
10	-	48 / 16	-	11	0.1	128	100
11	-	48 / 24	-		0.1	32	100
12	-	48 / 24	10–12 – 15–22	11	0.1	32	100

4. Results And Discussion

We compared the performance of the proposed architecture with two different machine learning models; the Support Vector Machine (SVM) and Naïve Bayes (NB) models. Table 9 and Table 8 report the experimental accuracy and loss function results. Table 8 summarises the accuracy and loss values of ten different deep learning models defined by different hyper-parameters, as shown in Table 7. Figure 10 presents an example for training and validation accuracy results over 100 training epochs.

Model 6 and Model 7 are chosen as optimum DNN models. The proposed models have used only 32 neurons for each hidden layer. The training dataset contains 48 samples, and the test dataset contains

16 samples. According to experimental results, the DNN performed better in test accuracy than the SVM and NB.

Table 9 represents the performance comparisons of DNN, SVM, and NB models in terms of train and test accuracy. Even though DNN has been modelled with only two hidden layers and without the need for feature engineering, it performed better than SVM and NB architectures, which are required to combine all features.

The proposed model was also tested using a random samples dataset to demonstrate the effect of position features on the surface roughness. As shown in Fig. 8, the distribution of the surface roughness value of each sample with random positions for each degree is over the threshold value and should be classified as 'ROUGH'. Random samples have been classified using the proposed DNN model, which is trained by using the same hyperparameters, except for the training and test sets. The training set includes 64 samples, and the test set includes 24 randomly positioned samples. According to the experimental results, our proposed model predicted 24 different randomly positioned samples as 'ROUGH' (see Table 10) as expected.

Table 8
Experimental results for DNN model with different hyper-parameters.

DNN Model Number	Training Accuracy	Validation Accuracy	Test Accuracy	Training Loss	Validation Loss	Test Loss
1	0.959	1.000	1.000	0.132	0.036	0.008
2	0.948	1.000	1.000	0.152	0.029	0.042
3	0.886	1.000	0.625	0.266	0.087	0.570
4	0.885	1.000	0.625	0.268	0.087	0.541
5	0.885	1.000	0.625	0.270	0.086	0.609
6	**0.958**	**-**	**1.000**	**0.244**	**-**	**0.000**
7	**0.958**	**-**	**1.000**	**0.041**	**-**	**0.000**
8	0.854	-	0.937	0.145	-	0.062
9	0.958	-	1.000	0.041	-	0.000
10	0.854	-	0.937	0.145	-	0.062

Table 9
Performance comparisons of the DNN, SVM and NB models in terms of training and test accuracy.

Model Name / Labelling Approach	Features	Mean Training Accuracy	Mean Test Accuracy
DNN without EOS© Labelling	-	0.958	**1.000**
DNN with EOS© Labelling	-	0.958	**1.000**
SVM with EOS© Labelling	All features	0.960	0.890
SVM without EOS© Labelling	All features	0.830	0.780
Naïve Bayes with EOS© Labelling	All features	0.920	0.850
Naïve Bayes without EOS© Labelling	All features	0.940	0.850

Table 10
Performancee results of the DNN model are tested using random positioned samples.

Model Name / Labelling Approach	Training Dataset	Test Dataset (Random Positions)	Mean Training Accuracy	Mean Test Accuracy.
DNN with EOS© Labelling	64	12	0.968	**1.000**
DNN without EOS© Labelling	64	12	0.875	**1.000**
DNN with EOS© Labelling	64	24	0.968	**1.000**
DNN without EOS© Labelling	64	24	0.875	**1.000**

5. Conclusion

This study proposes a new dataset and a model to estimate surface roughness, and results are presented. The powderbed technology yields many promising results with deficiencies. Production planning is one of the challenging subjects in the field. Finding a proper orientation is still a mounting and labour intensive task in the process. The surface roughness problem is addressed concerning part positions and orientations. A comprehensive dataset is created to represent the production process of the EOS Formiga P110 system. Then, the dataset is employed by a new estimation model based on DNN. The dataset and the model provide a new user interface to estimate the surface roughness of the product depending on coordinates in production space and other production parameters in the production planning phase. The results show that the new interface performs well for the production planning phase while only considering the surface roughness.

Declarations

Authors contributions: Ebubekir Koç: Research main theme, data preparation, algorithm design and implementation and experimental studies; Sultan Zeybek: Data preprocessing and Deep Learning Networks implementation; Burçin Özbay Kısasöz: SLS production parameters determination, characterization studies; Cemal İrfan Çalışkan: The sample design process and CAD modeling; M.Enes Bulduk: Production planning, SLS production and postprocess.

Funding: This study was carried out using the infrastructure and research funding provided by the ALUTEAM - Aluminum Test Training and Research Center of Fatih Sultan Mehmet Vakif University. The research infrastructure is supported by the Istanbul Development Agency (ISTKA) and the T.R. Ministry of Industry and Technology.

Availability of data and material: The authors confirm that the data and material supporting the findings of this work are available within the article.

Competing interests: The authors have no competing interests or conflicts of interest to declare that are relevant to the contents of this article.

Ethical approval: The article follows the guidelines of the Committee on Publication Ethics (COPE) and involves no studies on human or animal subjects.

Consent to participate: Not applicable. The article involves no studies on humans.

Consent to publish: Not applicable. The article involves no studies on humans.

References

1. Stansbury JW, Idacavage MJ. 3D printing with polymers: Challenges among expanding options and opportunities. Dent Mater [Internet]. 2016;32(1):54–64. Available from: http://dx.doi.org/10.1016/j.dental.2015.09.018
2. Bekem A, Özbay B, Bulduk M. Seçici laser sinterlemede poliamid 12'ye dendritik bakır tozu ilavesinin etkisi. Gazi Üniversitesi Mühendislik-Mimarlık Fakültesi Derg. 2020;1:421–31. https://doi.org/10.17341/gazimmfd.728198
3. Kumar S. Selective Laser Sintering: A Qualitative and Objective Approach. Jom. 2003;55(10):43–7. https://doi.org/10.1007/s11837-003-0175-y
4. Wroe WW. Improvements and effects of thermal history on mechanical properties for polymer selective laser sintering (SLS). 2015.
5. Çalışkan Cİ, Koç E. Kuşevleri ve 3 Boyutlu Baskı Yöntemi ile Üretimi. FSM İlmî Araştırmalar İnsan ve Toplum Bilim Derg. 2019; (13): 113–31. https://doi.org/10.16947/fsmia.582347
6. Schmid M, Schmid M. LS Materials Table. Laser Sinter with Plast. 2018;191–4.

7. Schmid M, Wegener K. Additive Manufacturing: Polymers applicable for laser sintering (LS). Procedia Eng. 2016;149:457–64. https://doi.org/10.1016/j.proeng.2016.06.692
8. Negi S, Dhiman S, Sharma RK. Investigating the Surface Roughness of SLS Fabricated Glass-Filled Polyamide Parts Using Response Surface Methodology. Arab J Sci Eng. 2014;39(12):9161–79. https:// doi.org/10.1007/s13369-014-1434-7
9. Schmid M, Schmid M. LS Process. Laser Sinter with Plast. 2018;39–64.
10. Ho HCH, Gibson I, Cheung WL. Effects of energy density on morphology and properties of selective laser sintered polycarbonate. J Mater Process Technol. 1999;89–90:204–10. https://doi.org/10.1016/S0924-0136(99)00007-2
11. Forster AM. Materials Testing Standards for Additive Manufacturing of Polymer Materials. Prog Addit Manuf. 2015;1:9–20.
12. Bodaghi, M., Mobin, M., Ban, D., Lomov, S. V., Nikzad, M., Surface quality of printed porous materials for permeability rig calibration. Materials and Manufacturing Processes (2021) 1-11. https://doi.org/10.1080/10426914.2021.1960994
13. Taufik, M., Prashant, K. J., Laser-assisted finishing process for improved surface finish of fused deposition modelled parts. Journal of Manufacturing Processes, 30 (2017) 161–177. https://doi.org/10.1016/j.jmapro.2017.09.020
14. G. F. Gomes, Y. A. D. Mendéz, P. da Silva Lopes Alexandrino, S. S. da Cunha, and A. C. Ancelotti, "The use of intelligent computational tools for damage detection and identification with an emphasis on composites – A review" Composite Structures. 2018.
15. S. Zeybek, "Remaining Useful Life Prediction of Engines for Remanufacturing using the Bees Algorithm Optimised Semi-Supervised Deep Learning Model" (pp. 517-552), Intelligent Production and Manufacturing Optimisation: The Bees Algorithm Approach. Springer, 2021.
16. Arafat, M., Sjafrizal, T. & Anugraha, R.A. An artificial neural network approach to predict energy consumption and surface roughness of a natural material. SN Appl. Sci. 2, 1174 (2020). https://doi.org/10.1007/s42452-020-2987-6.
17. Eva C. Hofland, Ismet Baran, Dagmar A. Wismeijer, "Correlation of Process Parameters with Mechanical Properties of Laser Sintered PA 12 Parts", Advances in Materials Science and Engineering, vol. 2017, Article ID 4953173, 11 pages, 2017. https://doi.org/10.1155/2017/4953173.
18. C. İ. Çalışkan, M. Coşkun, G. Özer, E. Koç, T. A. Vurkır, and G. Yöndem, "Investigation of manufacturability and efficiency of microchannels with different geometries produced by direct metal laser sintering" Int. J. Adv. Manuf. Technol., 2021. https://doi.org/10.1007/s00170-021-07928-0
19. Agrawal, A., Choudhary, A., 2019. Deep materials informatics: Applications of deep learning in materials science. MRS Communications 9, 779–792. https://doi:10.1557/mrc.2019.73.

Figures

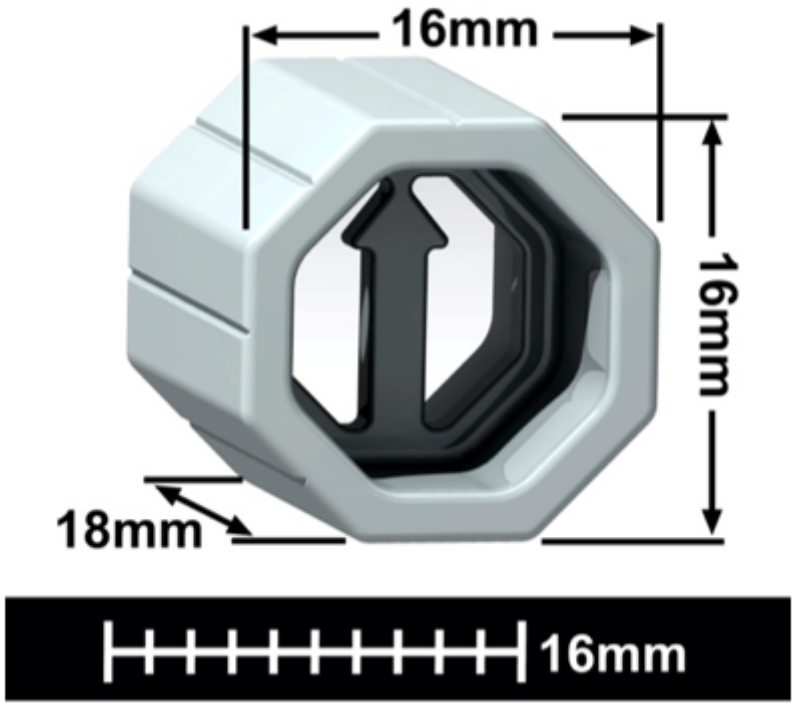

Figure 1

An octagonal test specimen is presented with 16mm x 16mm x 18mm, XYZ respectively.

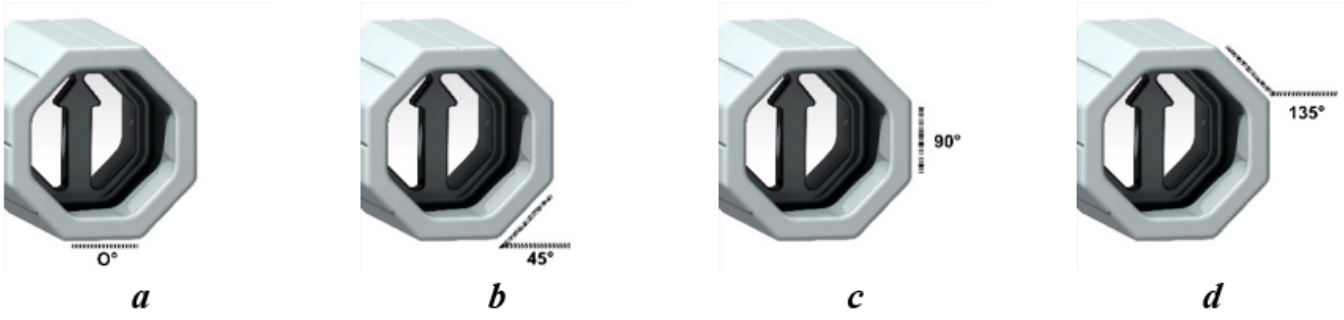

Figure 2

The measurements of the surface quality are carried out at surfaces a, b, c and d with the angels 0°, 45°, 90° and 135° respectively.

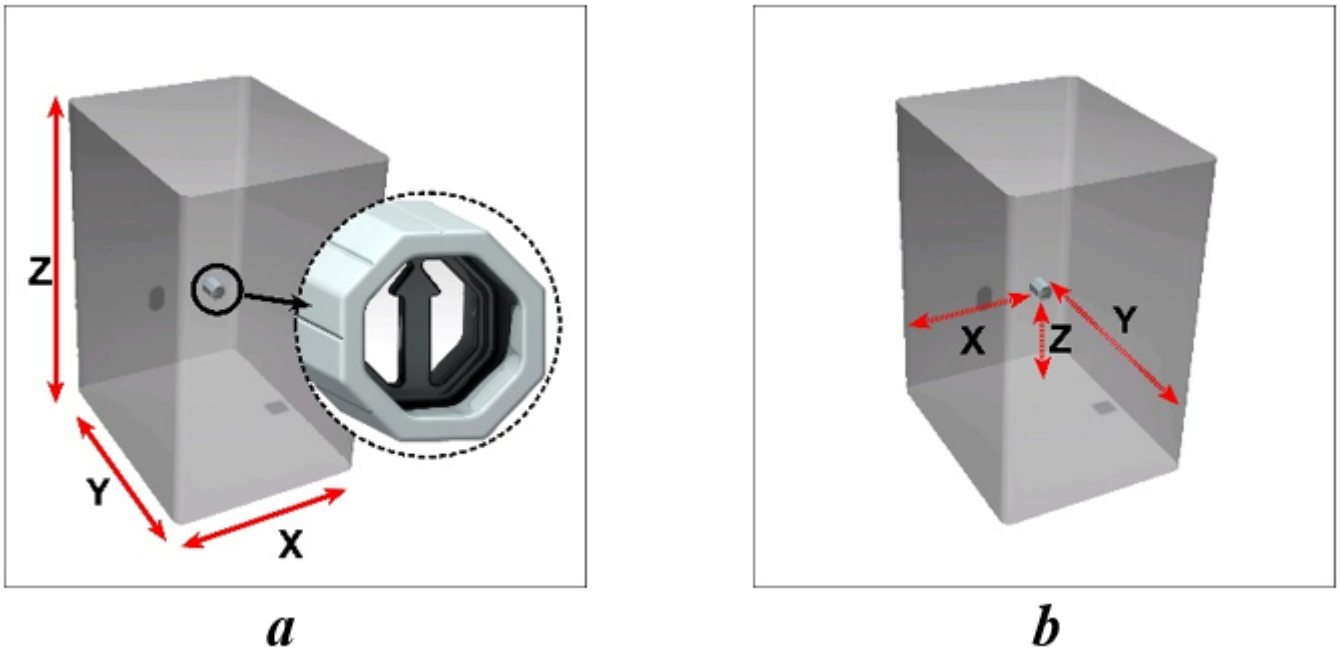

Figure 3

a. The production platform and dimensions of SLS technology are carried out in the research; x:192 mm, y:242 mm, z:320 mm, b. measurement method of x, y, z position information of test samples given in *Table 3*.

Figure 4

Preliminary results of mean surface roughness for 0^0 and 180^0 surfaces compare to original (EOS) parameters.

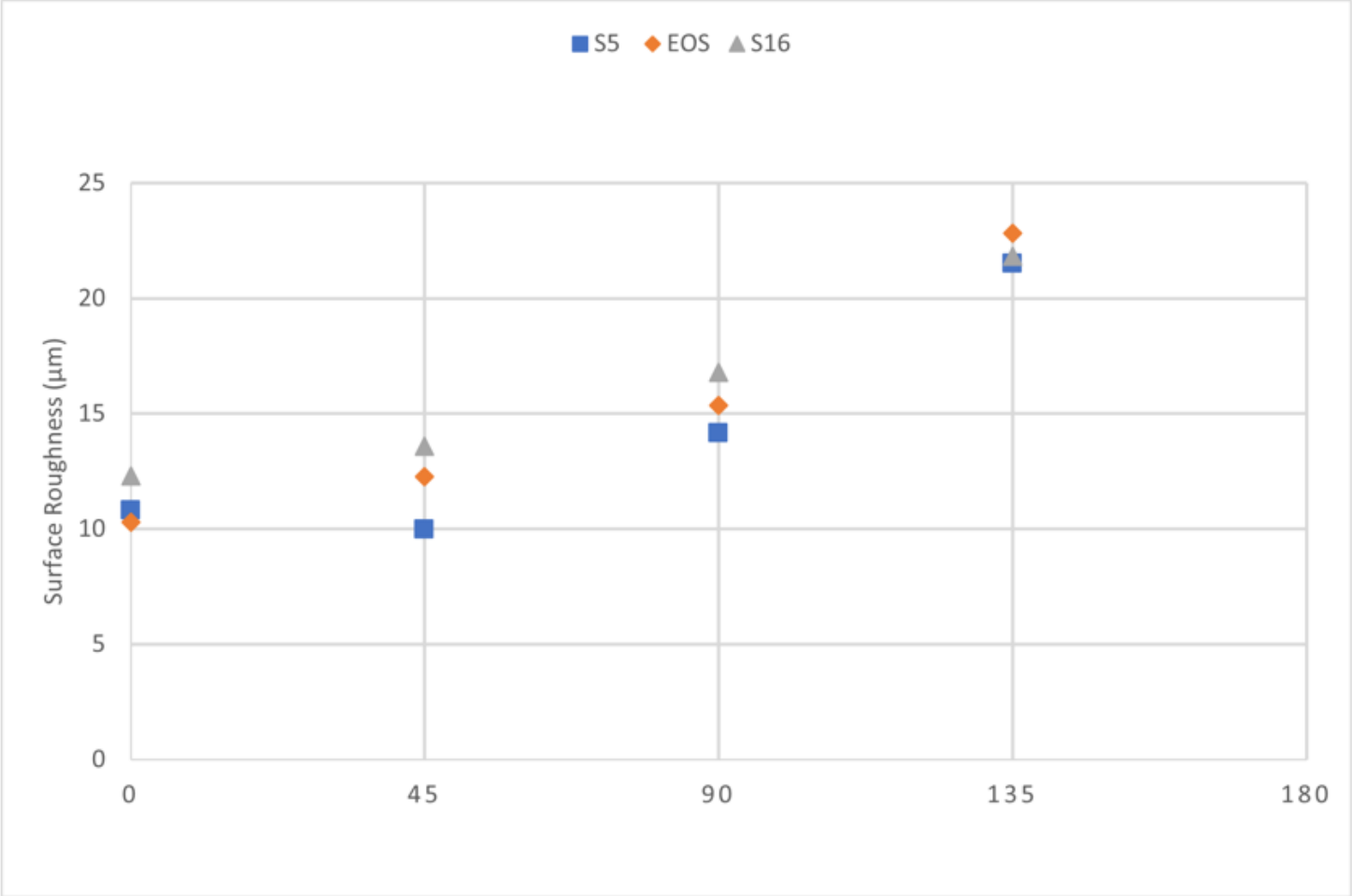

Figure 5

Surface roughness values of standard contour processing parameters parts.

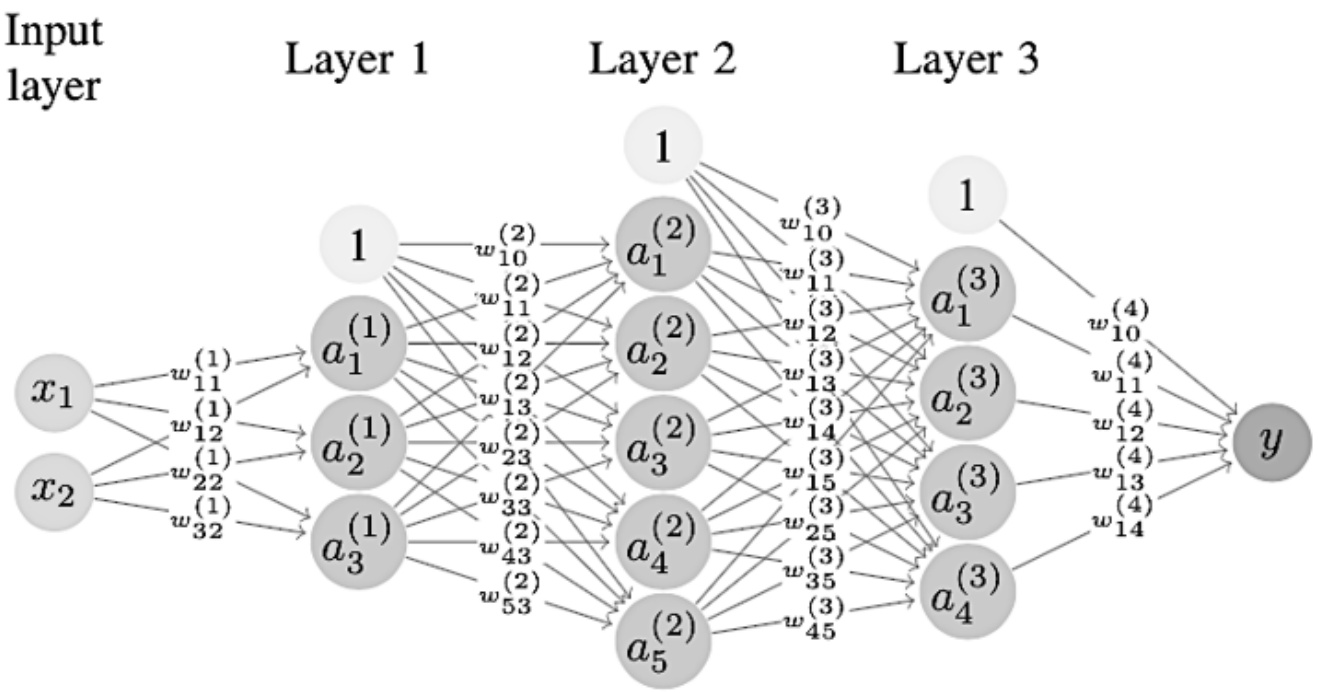

Figure 6

A DNN architecture combines an input layer, three hidden layers, and an output layer.

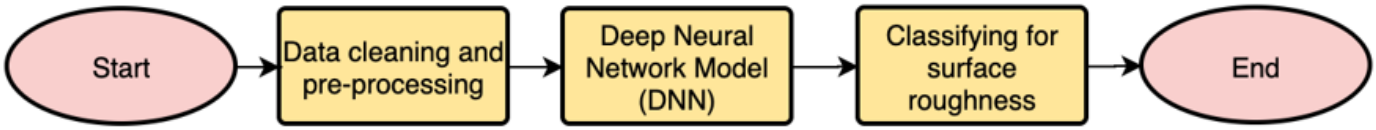

Figure 7

The pipeline of the proposed DNN model.

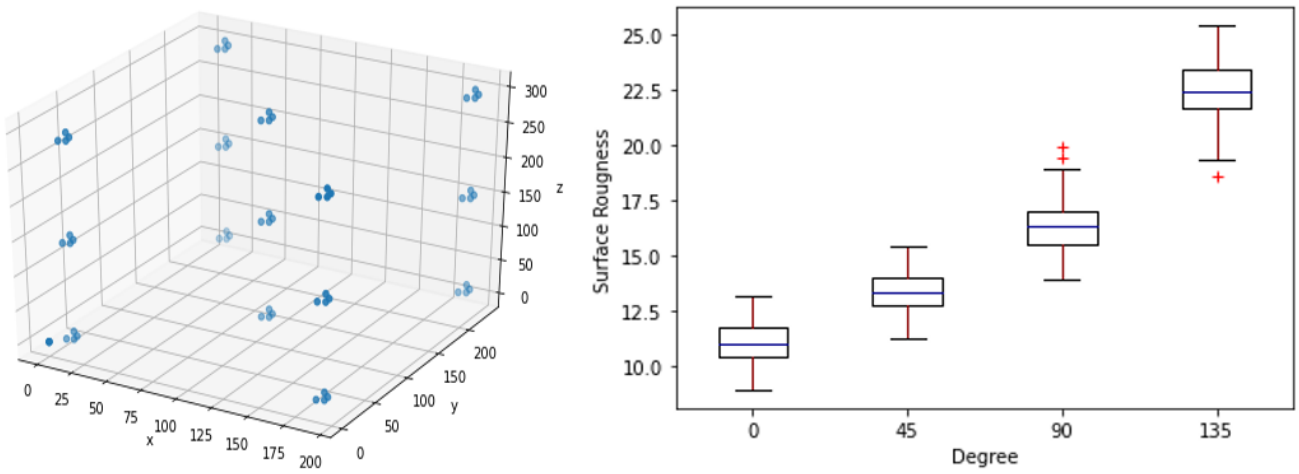

Figure 8

The distributions of the surface roughness measurement for three independent experiments of 15 samples each have different positions (left).

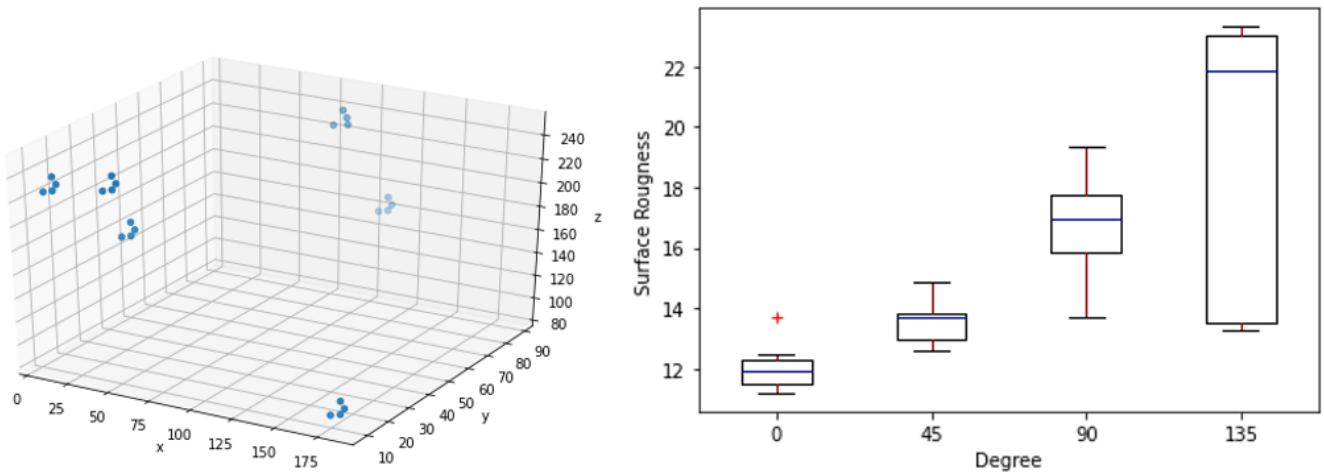

Figure 9

The distributions of the surface roughness measurement for three independent experiments of 6 randomly positioned samples for each angle, including 0, 45, 90, and 135 degrees (left).

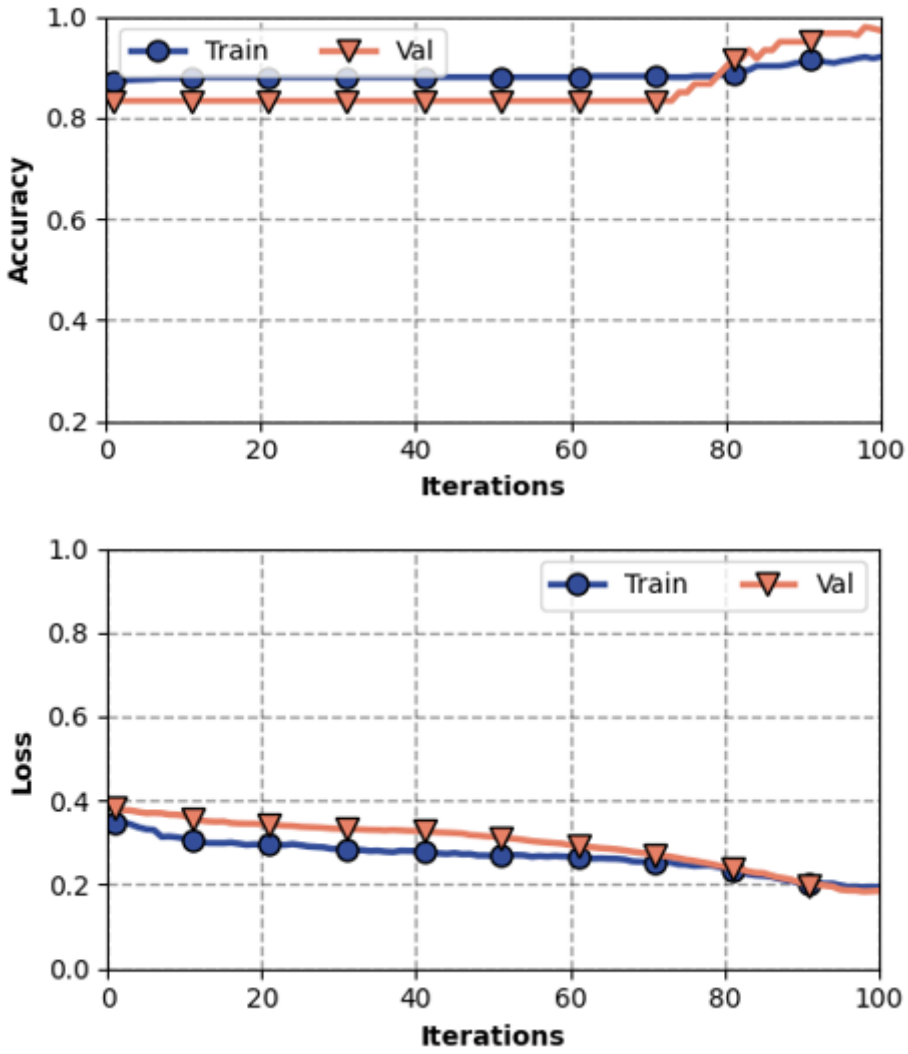

Figure 10

An example accuracy and loss results for train and validation dataset of DNN model.